https://ntrs.nasa.gov/search.jsp?R=19930084677 2020-06-17T18:53:28+00:00Z

NACA TN 3862 0225 5220

TECH LIBRARY KAFB, NM
0066775

NATIONAL ADVISORY COMMITTEE FOR AERONAUTICS

TECHNICAL NOTE 3862

DETERMINATION OF THE STRUCTURAL DAMPING COEFFICIENTS OF SIX FULL-SCALE HELICOPTER ROTOR BLADES OF DIFFERENT MATERIALS AND METHODS OF CONSTRUCTION

By Frederick W. Gibson

Langley Aeronautical Laboratory
Langley Field, Va.

AFMDC Technical Library
AFL 2811

NACA

Washington
December 1956

AFMDC
TECHNICAL LIBRARY
AFL 2811

TECH LIBRARY KAFB, NM
0066775

NATIONAL ADVISORY COMMITTEE FOR AERONAUT

TECHNICAL NOTE 3862

DETERMINATION OF THE STRUCTURAL DAMPING COEFFICIENTS OF SIX FULL-SCALE HELICOPTER ROTOR BLADES OF DIFFERENT MATERIALS AND METHODS OF CONSTRUCTION

By Frederick W. Gibson

SUMMARY

Measurements were made of the internal or structural damping characteristics of six full-scale helicopter rotor blades of six different materials and methods of construction. Structural damping coefficients are presented for the first three flapwise bending modes, the first torsion mode, and the first chordwise bending mode for all blades.

The structural damping coefficients for all blades are presented in tabular form together with the frequencies, amplitudes of oscillation, and approximate stresses in flapwise bending. Approximate torsional stresses are also given for one blade. Typical samples of the data are plotted to show effects of material of construction, mode shape, and amplitude on the structural damping coefficients.

The contribution of structural damping to the total damping of the blades is discussed for several aerodynamic conditions in order to point out situations where structural damping is significant.

INTRODUCTION

Helicopter-rotor-blade vibration problems of fundamental importance can be grouped into two general categories: forced vibrations and self-excited vibrations. In the case of forced vibration (the category investigated herein), there are ranges of rotor speed where harmonics of the aerodynamic loading, which have frequencies equal to integral multiples of the rotor speed, produce large blade deflections and stresses. It has been observed, both analytically and experimentally, that this phenomenon usually arises because of resonance amplification and occurs at rotor speeds where the frequencies of the harmonics of aerodynamic loading are equal or nearly equal to the various natural frequencies of the coupled blade-fuselage structure. For most practical helicopter applications, the significant modes are those that involve substantial

amounts of blade bending. One of the factors which influence the amplitudes of these vibrations is the internal or structural damping of the rotor blades. Ratios of known values of structural damping to total damping for wings and similar built-up structures were obtained by assuming quasi-static aerodynamic damping or by applying two-dimensional potential-flow theory for wings oscillating in bending only. A comparison of these ratios indicates that the contribution of structural damping to the total damping is small. However, recent analytical studies (for example, ref. 1) showed that consideration of the helical wake pattern, which is made up of vortices shed by previous passages of all blades of the rotor, may lead to conditions in which the aerodynamic damping becomes extremely low if the rotor inflow is small and if the blade is vibrating at a frequency which is an integral multiple of the rotor frequency. If the natural frequency of one or more of the bending modes of the rotating blade is equal to one or more of the harmonics of the rotor speed, conditions of resonance exist, together with conditions for low aerodynamic damping and, in this case, structural damping becomes of much greater importance in limiting the amplitudes of blade response.

Inasmuch as conditions are indicated in which the role of structural damping in helicopter-rotor-blade vibrations may be important, it seemed appropriate that measurements be made with existing full-scale helicopter rotor blades of various types and materials of construction in order to determine the extent of variation of structural damping achieved in design practice. Consequently, damping measurements were made on six different rotor blades and the results are presented herein.

The data presented show the variation of damping with material and type of construction, frequency, mode shape, and amplitude. An approximate comparison is made of the magnitude of structural damping relative to the aerodynamic damping predicted by oscillating-airfoil theory without consideration of the helical wake pattern of the rotating blades, and the relative importance of the structural damping for the more realistic case of the helical wake is discussed.

SYMBOLS

a_o	initial amplitude of portion of decrement under consideration
a_n	amplitude of nth cycle of portion of decrement under consideration
f	natural frequency, cps

g	structural damping coefficient, $\frac{\log_e \frac{a_o}{a_n}}{\pi n}$
g_t	total damping coefficient (aerodynamic damping plus structural damping)
h_1, h_2, h_3	first, second, and third flapwise bending modes
h_c	first chordwise bending mode
α	first torsion mode
m	mass per unit length of blade, lb-sec^2/in.^{2}
m_r	mass per unit length of blade at root, lb-sec^2/in.^{2}
n	integral number
σ	maximum bending stress, lb/sq in.
τ	maximum torsional stress, lb/sq in.
γ	strain, in./in.
x	spanwise coordinate of blade measured from root, in.
EI	bending stiffness of blade at x, lb-in.^{2}
EI_r	bending stiffness of blade at root, lb-in.^{2}
R	radius of rotor blade, in.

APPARATUS AND METHODS

Description of Blades

Pertinent details of the blades such as plan form, dimensions, and material used in construction of the skin are given in figure 1. The blades are identified in the figure by the numerals I to VI and this designation is used throughout the paper.

Testing Techniques

The blades were vibrated in their natural modes until the desired amplitude was reached, after which the exciting force was instantaneously

removed. The oscillations were permitted to decay and the decrement was recorded on oscillograph records by using the output of an accelerometer which was mounted at an appropriate location on the blade. A reproduction of a portion of a typical oscillograph record is shown in figure 2.

Mounting and excitation of blades.- In order to minimize the damping of the blade mounting attachments so as to study only the structural damping of the blades themselves, the methods of suspension were as follows:

1. For the flapwise bending modes, the blades were mounted to a rigid surface as shown in figure 3. The taut cable suspension at the root was used to minimize the support friction and to simulate a hinged condition at the root. The outboard support consisted of a wooden block attached to a long flexible cable, the block being cut with a double radius so that the bearing surface was essentially a point. This point was movable spanwise and, in the excitation of a given mode, was always placed at the outermost nodal point of the blade. The exciting force was applied perpendicular to the chord plane, its chordwise position approximately coincident with the first torsional node line and as close to the blade root as practicable.

2. For the chordwise bending mode, the blades were mounted as shown in figure 4. The method was essentially the same as that used for flapwise bending except that the blade was rotated 90°. The tip section was supported by a flexible cable attached to a bolt which passed through the blade at the spanwise position of the chordwise bending node. The exciting force was applied at the leading edge with its direction parallel to the chord line.

3. In order to obtain the damping in torsion, the blades were mounted with the root rigidly bolted to the mounting surface as shown in figure 5. The flexible cable supporting the outboard section was attached to the blade at the first torsional node line and the exciting force was applied normal to the chord plane at the trailing edge near the root.

Determination of damping coefficients.- From the oscillograph records the amplitudes and natural frequencies were obtained. The damping coefficients $\left(\text{defined as } g = \frac{\log_e \frac{a_o}{a_n}}{\pi n}\right)$ were obtained from logarithmic plots such as the one shown in figure 6.

Still-air damping.- The damping coefficients obtained from the decay of oscillation of the blades when mounted and shaken as previously described are subject to an aerodynamic correction because of the oscillatory motion of the blade with and relative to the air surrounding it.

This oscillatory motion is the limiting value of the aerodynamic damping when the forward translational velocity of the blade elements vanishes and is of interest primarily insofar as it affects the accuracy of the determination of the structural damping.

In order to determine the relative magnitude of this "still air" damping, blade VI was installed in a vacuum chamber and the damping coefficients were obtained at pressures of 14.7 and 0.245 pounds per square inch absolute. The difference in the damping values in the two mediums proved to be of the order of magnitude of the accuracy of the measurements (5 to 10 percent) and could not, therefore, be properly evaluated. At this level, the damping due to the still air surrounding the blade would seem to be of secondary importance.

Approximation of blade stresses.- As a point of interest and in order to obtain a practical basis on which to compare the damping values of the various modes for any one blade, the stresses in the skin at maximum amplitude were estimated for all blades.

The method used to estimate the blade bending stresses was as follows: The mass and stiffness distributions were assumed to be of the form $m = m_r(1 - x/2R)$ and $EI = EI_r(1 - x/2R)$, respectively, for blades I, II, III, and VI and to be uniform for blades IV and V. The tabulated modes, shapes, and curvatures for blades having these properties were obtained from reference 2 where they are given for specified deflections at various spanwise stations. Inasmuch as the curvature associated with a given natural mode is proportional to the deflection at any spanwise station, the curvatures d^2h_n/dx^2 and, hence, the strains associated with the measured deflections were readily obtained. Elementary beam theory was then applied to the section of maximum curvature to obtain stresses:

$$\sigma = E\frac{t}{2}\frac{d^2h_n}{dx^2}$$

where σ is the stress in the outermost fiber in pounds per square inch, E is the modulus of elasticity in bending in pounds per square inch, t is the maximum thickness in inches of the blade at the point of maximum curvature, and the subscript n denotes the mode in question.

In the case of torsion, the maximum torsional stress τ, measured in pounds per square inch, was approximated for the first mode of blade VI only and is given by $\tau = G\gamma$ where G is the modulus of elasticity in shear and γ is the shear strain measured experimentally.

RESULTS AND DISCUSSION

Presentation of Results

The complete results of the damping tests are presented in table I wherein are also given the measured values of damping, the ranges of amplitude for which the values apply, and the estimated stresses at maximum amplitude. Selected samples of these data are also plotted to emphasize some of the more significant effects observed.

The effect of amplitude on the structural damping is shown in figure 6. The effects of mode shape and amplitude or stress level on the structural damping are illustrated in figure 7, and the effects of material of construction are shown in figure 8.

Discussion of Results

Effect of amplitude.- A typical example of the manner in which the structural damping varies with amplitude is illustrated by the data presented in figure 6. The amplitudes of vibration of the various natural modes during the decay of the motion following the removal of the exciting forces are plotted as a function of the number of cycles in the decrement. The curves that connect the data points are the envelopes of the decrements. These data show that the slopes of the curves and, therefore, the structural damping remain constant over distinct ranges of the decrement, and for this reason this method was used in the presentation of the summary of the data in table I.

All curves shown in figure 6, which includes the first three elastic bending modes as well as the first elastic torsion mode for blade IV, indicate the general trend of a reduction in structural damping with a reduction in amplitude. This trend was also found for the flapwise bending and torsion of all the blades tested with the exception of the second bending mode of blade II, where an increase in structural damping with a decrease in amplitude was exhibited in one portion of the decay of oscillations. Two instances were also encountered in chordwise bending (blades IV and V, table I) in which the damping increased in a portion of the decrement as the amplitude diminished.

Effect of mode shape.- The effect of mode shape on the structural damping is shown in figure 7 where the structural damping coefficient is plotted as a function of blade stress. Figure 7(a) shows that for blade VI, at this stress level, there is little difference in the damping values for the flapwise bending modes, whereas the torsion mode exhibits structural damping of a much higher order of magnitude. Figure 7(b), which is plotted from the data for blade IV, indicates

the same trend as blade VI in the flapwise bending modes with respect to increase of structural damping with stress; however, in this case the variation of structural damping with mode shape is much greater than that for blade VI. The data presented in figure 7 and the other data in table I indicate no definite trend in the variation of structural damping with mode shape.

Effect of material of construction.- Since the data of the tests showed that the structural damping coefficients of the blades varied with amplitude of oscillation, a realistic basis was sought upon which to compare the damping in a given mode for all the blades. From the practical standpoint, strain seemed to be the most desirable basis for comparison and was, therefore, selected.

Figure 8 illustrates the effect of material of construction on the damping of all six blades vibrating in the first flapwise bending mode. The strain at the spanwise position of maximum curvature, based on a 1-inch tip deflection for blade I, is equal for all blades. On this basis the data indicate that blades III, V, and VI had somewhat higher damping coefficients than blades I, II, and IV.

Relative importance of aerodynamic and structural damping.- Results of analytical studies (ref. 3), in which quasi-static aerodynamic damping was assumed, showed that the difference between the peak values of blade response, with and without the inclusion of structural damping, was of the order of 6 percent of the peak value for the third elastic bending mode and was somewhat less for the first and second modes. The application of two-dimensional potential-flow theory for wings oscillating in bending only (ref. 4) yields somewhat smaller values of aerodynamic damping and also indicates that the contribution of structural damping to the total damping of the blade in bending is small. These data are presented in figure 9 and cover a frequency range which includes the first three natural flapwise bending modes of the fabric and stainless-steel blades with centrifugal stiffening effects included. The lines faired through the plotted points do not denote a linear increase in the ratio of structural damping to total damping with frequency but are only intended to indicate a trend.

The data presented in figure 9 are based on the assumption that the damping of a helicopter rotor blade can be calculated from wing theory for a wing having the properties of the blade element at 75 percent of the rotor blade radius (blade tangential velocity of 450 feet per second). This theory neglects the effects of the helical wake which is made up of vortices shed by previous passages of all blades of the rotor. The results of recent analytical studies (ref. 1) showed that consideration of the helical wake pattern leads to conditions in which the aerodynamic damping may become very low if the rotor inflow is small and if the blade is vibrating at a frequency equal to the frequency of

one or more of the harmonics of the rotor speed. In this case, structural damping becomes of much greater importance and an increase in structural damping could prove beneficial in reducing blade stresses and in increasing blade fatigue life.

The foregoing remarks are related to blade bending under forced excitation, although similar remarks are also pertinent to blade torsion. The most significant effects of structural damping, however, are expected to arise in the consideration of various instabilities such as wake flutter, classical flutter, and stall flutter. In these situations when the aerodynamic damping becomes negative, the amount of structural damping available may have a very significant effect on the flutter speed and on the magnitude of the flutter.

CONCLUDING REMARKS

On the basis of the damping measurements obtained for the six full-scale helicopter rotor blades of different materials and methods of construction and in consideration of studies made of the results of the investigation referred to in this paper, the following concluding remarks are made:

1. At the same strain levels, the rotor blades covered with fabric and wood materials had somewhat higher structural damping values in the first elastic bending mode than blades covered with metallic materials and fiber glass.

2. In the first three elastic bending modes and the first elastic torsion mode, all the blades exhibited an increase in structural damping with an increase in amplitude except for a portion of the amplitude range of the fiber glass blade vibrating in the second elastic bending mode. In the chordwise bending mode, the aluminum blade and one of the wood blades tested showed an increase in structural damping with a decrease in amplitude over a portion of the amplitude range.

3. No definite pattern or trend in the variation of structural damping with mode shape was exhibited.

4. Under normal operating conditions, in which blade bending motions are dominant, the contribution of structural damping to the total damping of rotor blades is shown to be small if the helical wake pattern is ignored. Consideration of the helical wake pattern, together with low rotor inflow at rotor speeds where a natural frequency of the rotor blade equals a harmonic of the rotor speed, may result in very low aerodynamic damping in which case the internal or structural damping of the rotor blade will assume a significant role in limiting the response of

the blade to exciting forces. Thus, the selection of materials with high structural damping would appear to merit consideration in the design of rotor blades.

Langley Aeronautical Laboratory,
National Advisory Committee for Aeronautics,
Langley Field, Va., August 29, 1956.

REFERENCES

1. Loewy, Robert G.: A Two-Dimensional Approximation to the Unsteady Aerodynamics of Rotary Wings. Preprint No. 605, S.M.F. Pub. Fund Preprint, Inst. Aero. Sci., Jan. 1956.

2. Yntema, Robert T.: Simplified Procedures and Charts for the Rapid Estimation of Bending Frequencies of Rotating Beams. NACA TN 3459, 1955. (Supersedes NACA RM L54G02.)

3. Daughaday, H., and Kline, J.: An Approach to the Determination of Higher Harmonic Rotor Blade Stresses. Rep. No. CAL-52, Cornell Aero. Lab., Inc., Mar. 1953.

4. Theodorsen, Theodore, and Garrick, I. E.: Mechanism of Flutter - A Theoretical and Experimental Investigation of the Flutter Problem. NACA Rep. 685, 1940.

TABLE I.- SUMMARY OF DAMPING DATA

Blade	Root chord, ft	Chord at 0.75R, ft	Weight, lb	Data for modes - h_1				h_2				h_3				α				h_c		
				f, cps	Stress in skin at max. amplitude, σ, lb/sq in.	Tip amplitude range, in.	g	f, cps	Stress in skin at max. amplitude, σ, lb/sq in.	Tip amplitude range, in.	g	f, cps	Stress in skin at max. amplitude, σ, lb/sq in.	Tip amplitude range, in.	g	f, cps	Stress in skin at max. amplitude, τ, lb/sq in.	Tip amplitude range, in.	g	f, cps	Tip amplitude range, in.	g
I	2	1.7	125	6.67	6,000	1.12 to .5[a]	0.01	18.8	4,100	0.29 to .16	0.0058	36.5	5,620	0.2 to .09	0.006	30.6	—	0.29 to .126	0.014	25.9	0.25 to .10	0.014
						.5[a] to .3	.005			.16 to .08	.0037			.09 to .05	.0046			.126 to .05	.007		.10 to (a)	.010
						.3 to (a)	.005							.05 to (a)	.005			.05 to .02	.006			
																		.02 to .015	.005			
II	2	1.8	125	5.5	1,272	2.8 to 1.41	.022	14.8	255	.251 to .07	.007	28.9	800	.397 to .104	.009	29.2	—	.18 to .04	.02	25.8	.207 to .06	.01
						1.41 to .75	.010			.07 to .037	.005			.104 to .0155	.006			.04 to .007	.005		.06 to (a)	.0086
						.75 to .3	.006			.037 to .015	.006											
III	2	1.7	120	4.1	590	1.57 to .25	.0125	10.4	350	.327 to .087	.0118	20.4	850	.39 to (a)	.012	25.8	—	.68 to .025	.027	14.8	.284 to .055	.027
						.25 to (a)	.009			.087 to .039	.009										.055 to (a)	.020
IV	1.37	1.37	116	4.8	2,200	1.2 to .36	.011	13.6	2,200	.4 to .06	.008	27.6	3,000	.25 to .066	.023	27.8	—	.28 to .066	.011	18.7	.075 to .014	.057
						.36 to .19	.0067			.06 to .04	.0066			.066 to .034	.011			.066 to .03	.008		.014 to .011	.019
														.034 to .020	.0057			.03 to .012	.006		.011 to (a)	.057
V	1.37	1.37	100	4.2	1,340	4.57 to 2.45	.02	13.8	417	.42 to (a)	.009	29.1	550	.287 to .04	.01	27.5	—	.308 to .055	.018	17.1	.14 to .02	.026
						2.45 to .9	.012							.04 to (a)	.009			.055 to .02	.013		.02 to .006	.021
						.9 to (a)	.009														.006 to (a)	.054
VI	1.29	1.0	100	5.5	915	2.28 to 1.0	.013	16.7	470	.57 to .078	.0077	34.3	525	.2 to .04	.01	37.6	396	.197 to .05	.027	19.7	.259 to .055	.014
						1.0 to .42	.009			.078 to (a)	.006			.04 to (a)	.006			.05 to (a)	.014		.055 to (a)	.009
						.42 to (a)	.0065															

[a]Denotes to smallest amplitude measured.

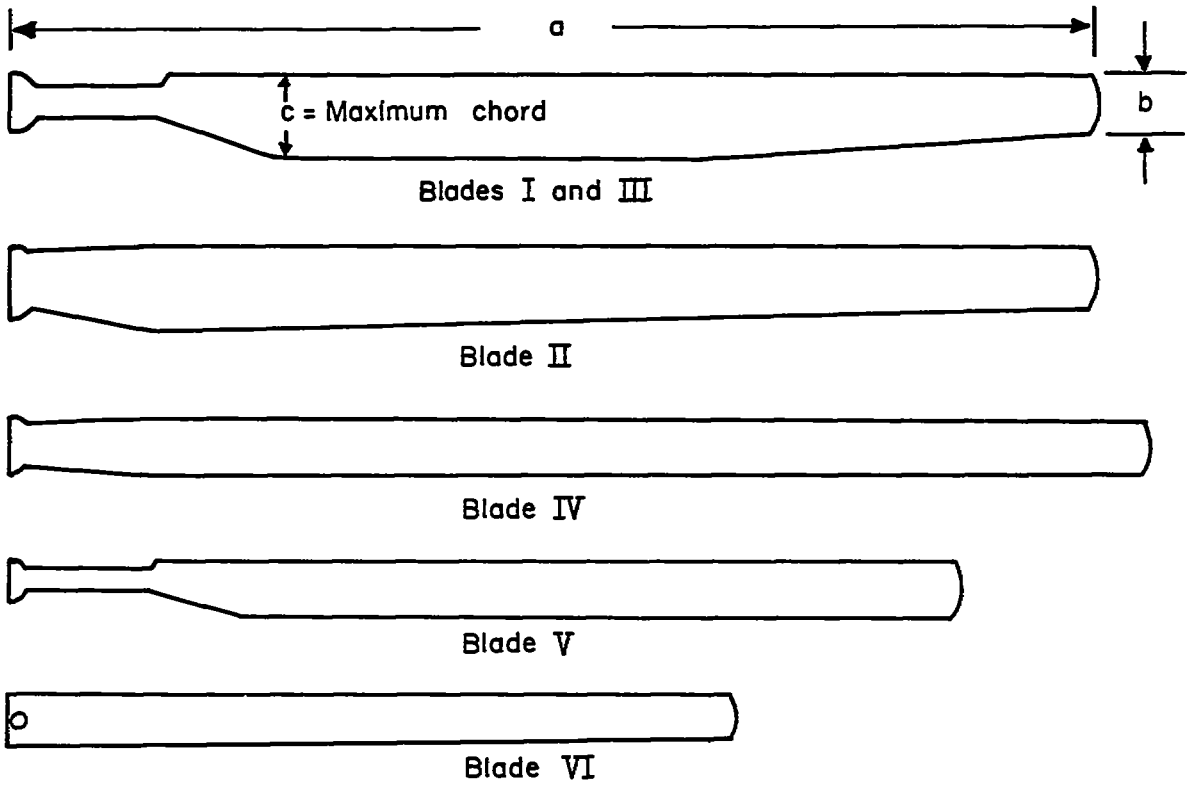

Blade	Material	Dimensions, in.			Weight, lb
		a	b	c	
I	Stainless steel	260	16	24	125
II	Fiber glass	260	16	24	125
III	Fabric	260	16	24	120
IV	Aluminum	266	16.5	16.5	116
V	Wood	233	16.5	16.5	100
VI	Wood	214	11	15.5	100

Figure 1.- Details of test blades.

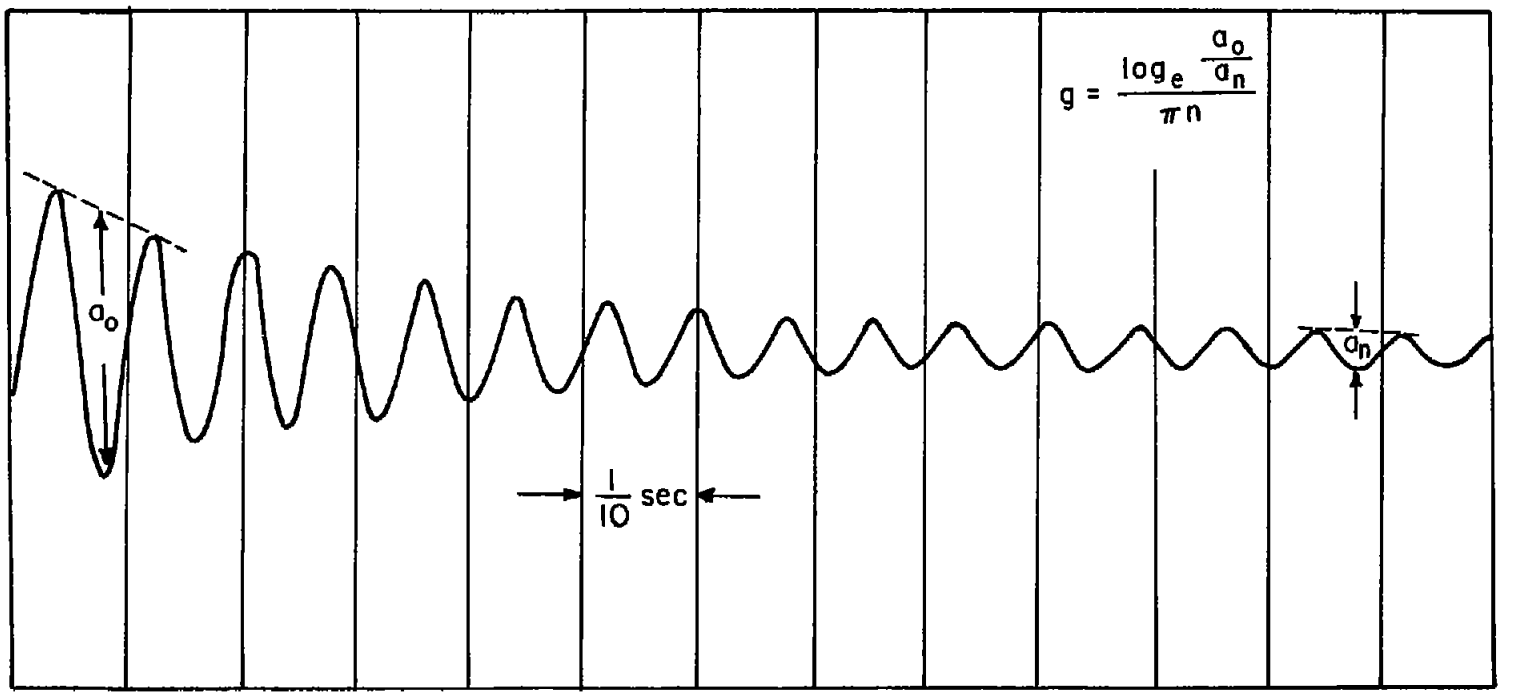

Figure 2.- Reproduction of a portion of a typical oscillograph record.

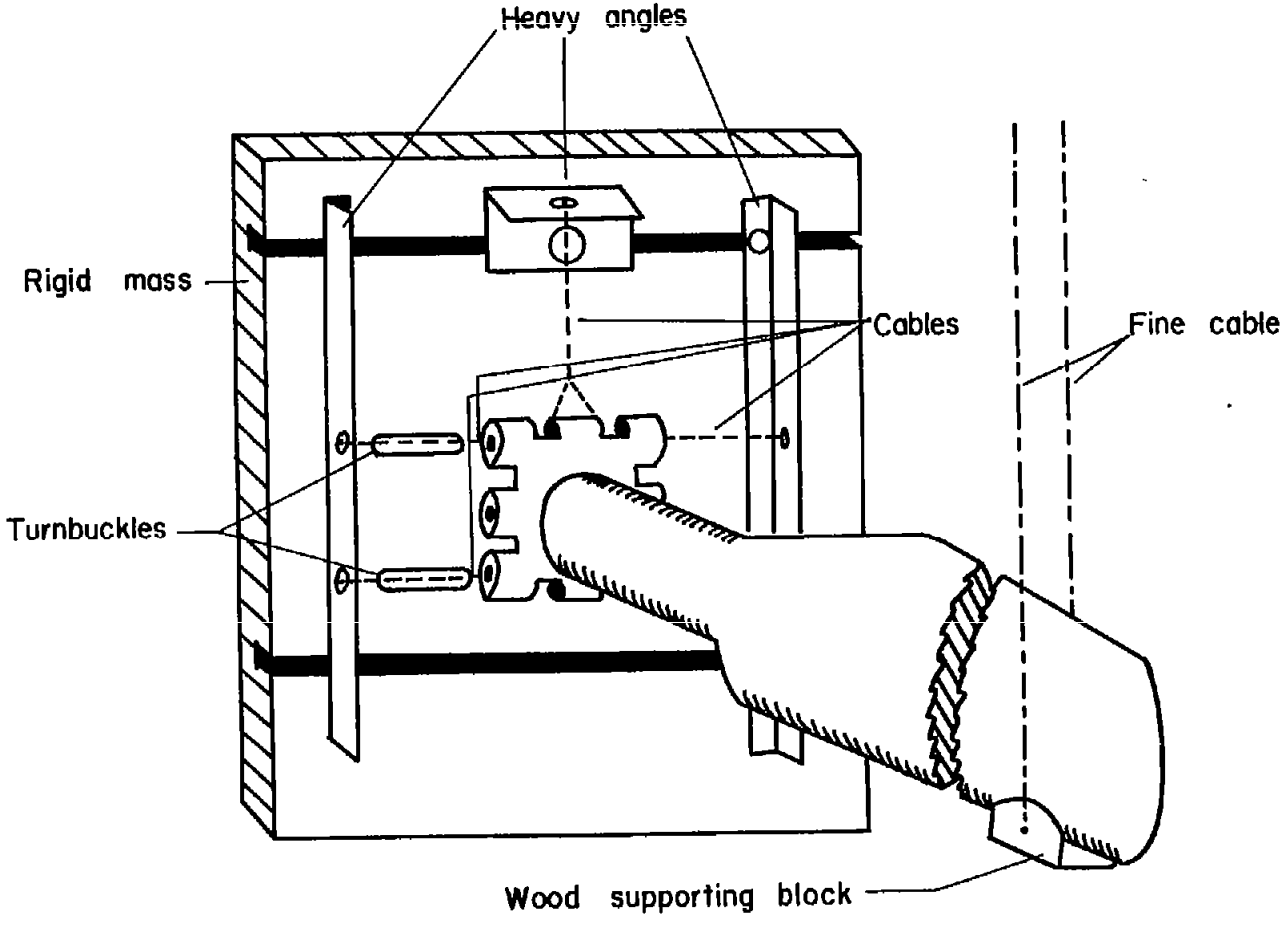

Figure 3.- Mounting of blades for flapwise bending.

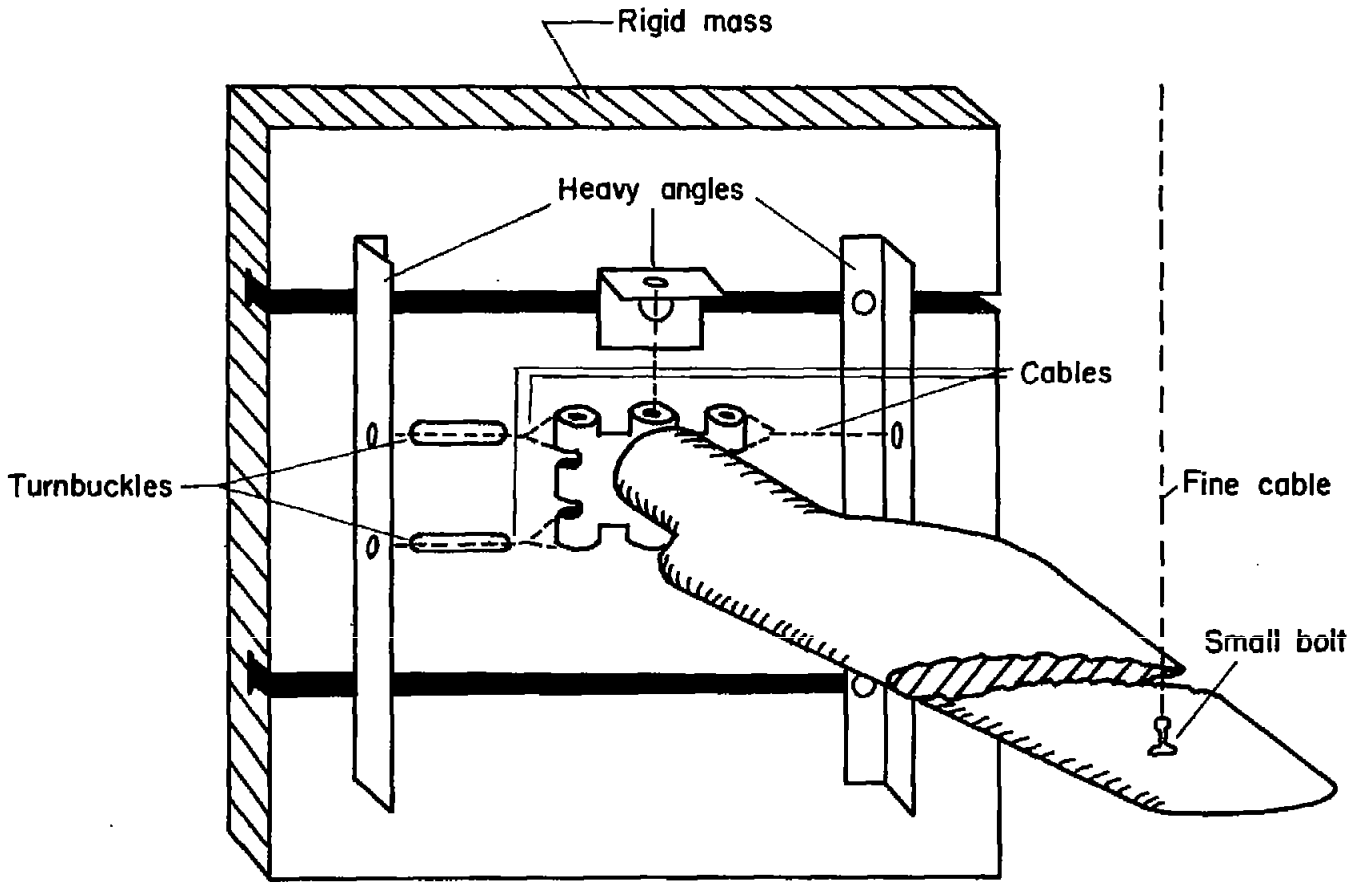

Figure 4.- Mounting of blades for chordwise bending.

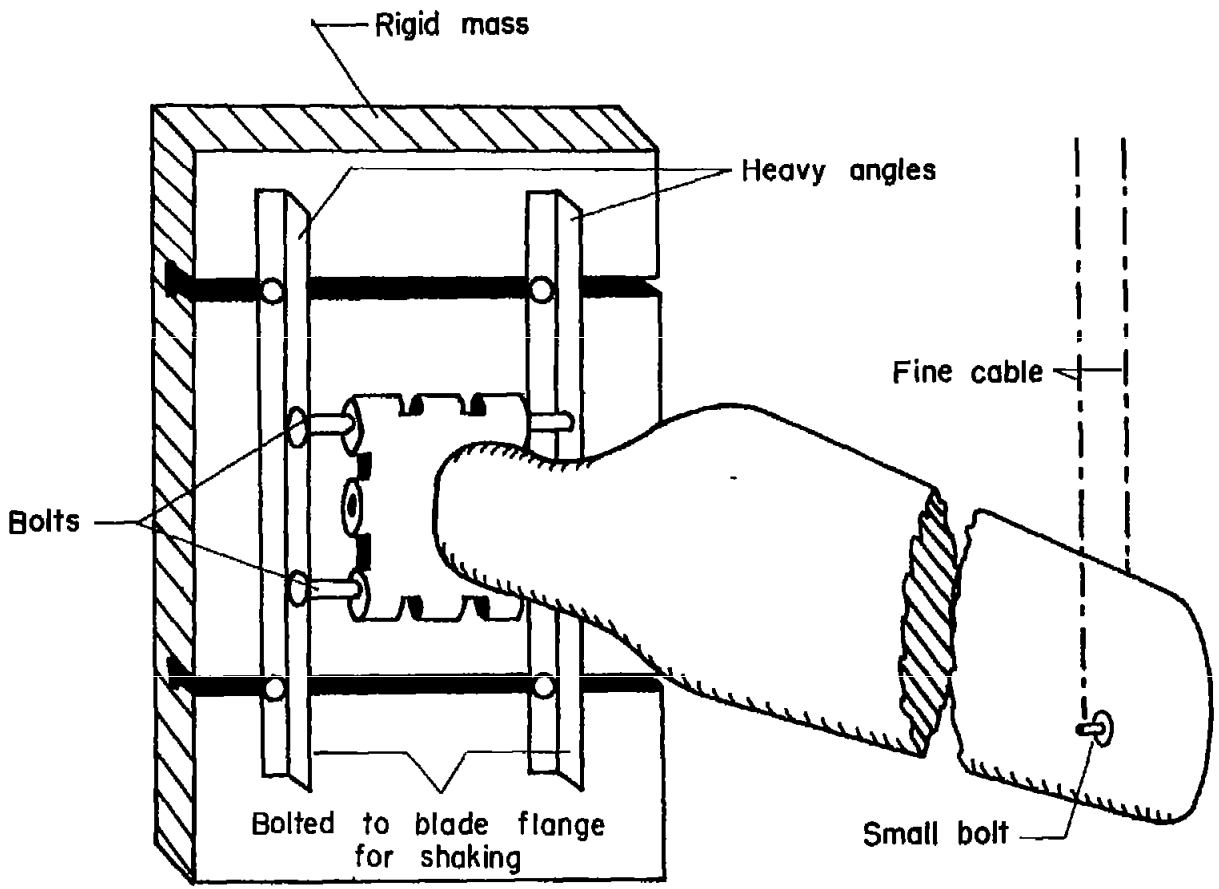

Figure 5.- Mounting of blades for torsion.

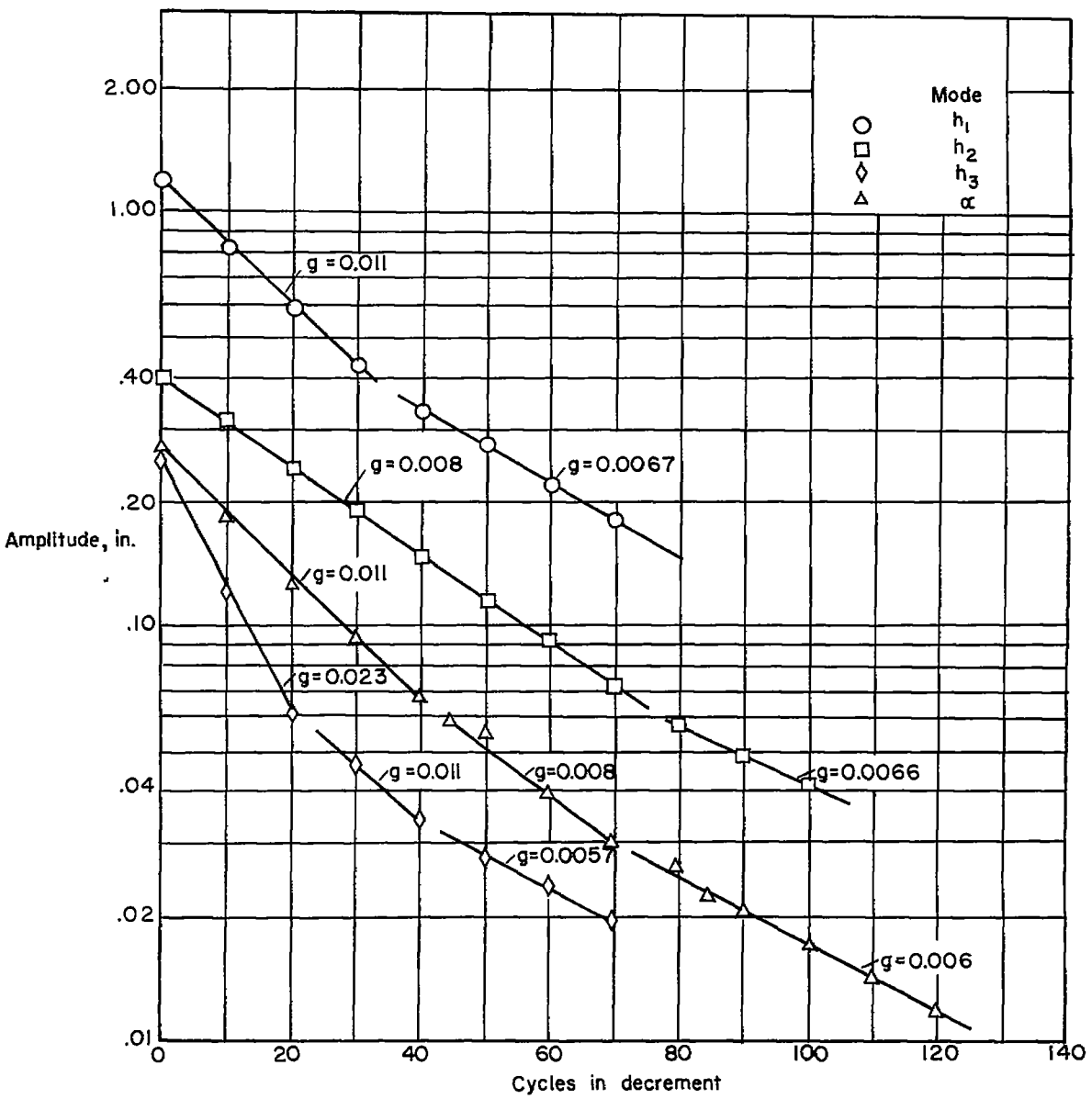

Figure 6.- Effect of amplitude on damping. Blade IV vibrating in flapwise bending and torsion.

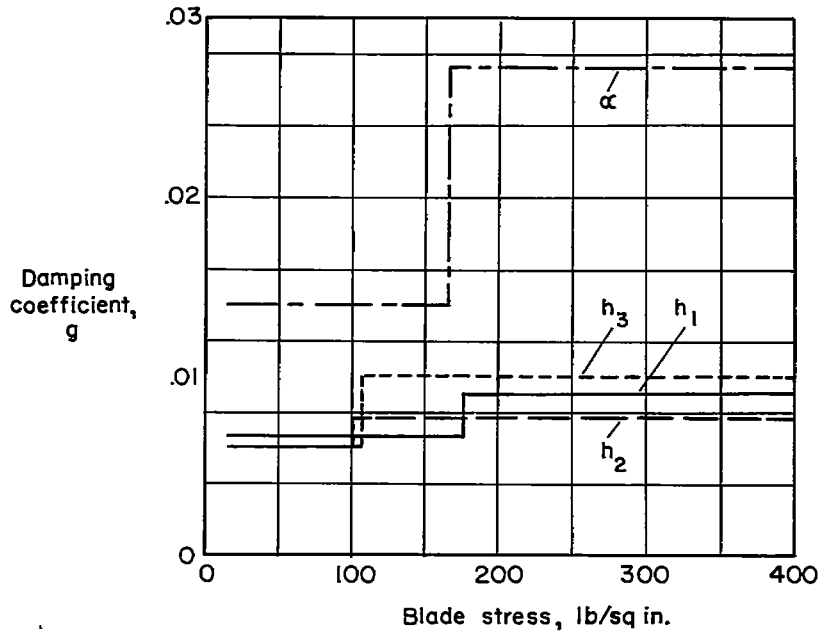

(a) Blade VI.

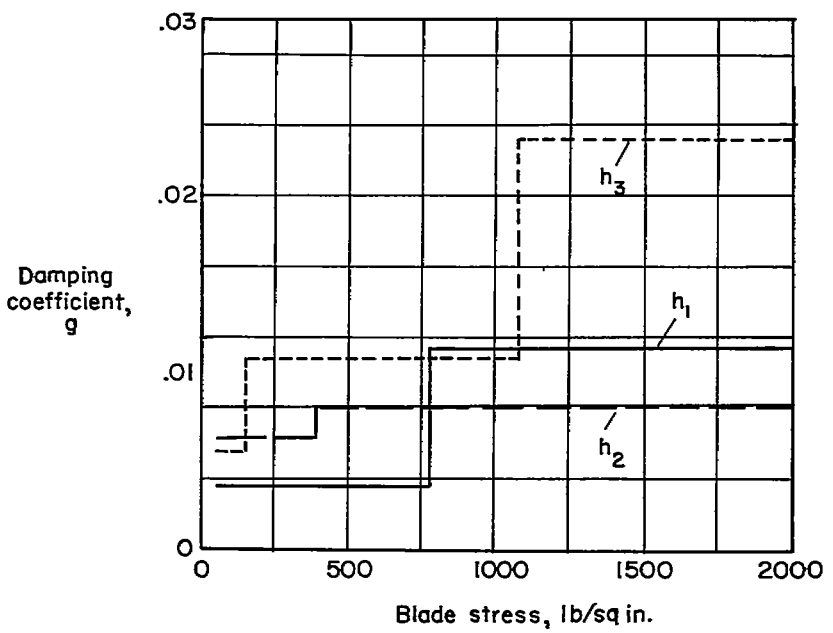

(b) Blade IV.

Figure 7.- Variation of structural damping with mode shape and amplitude (or stress level).

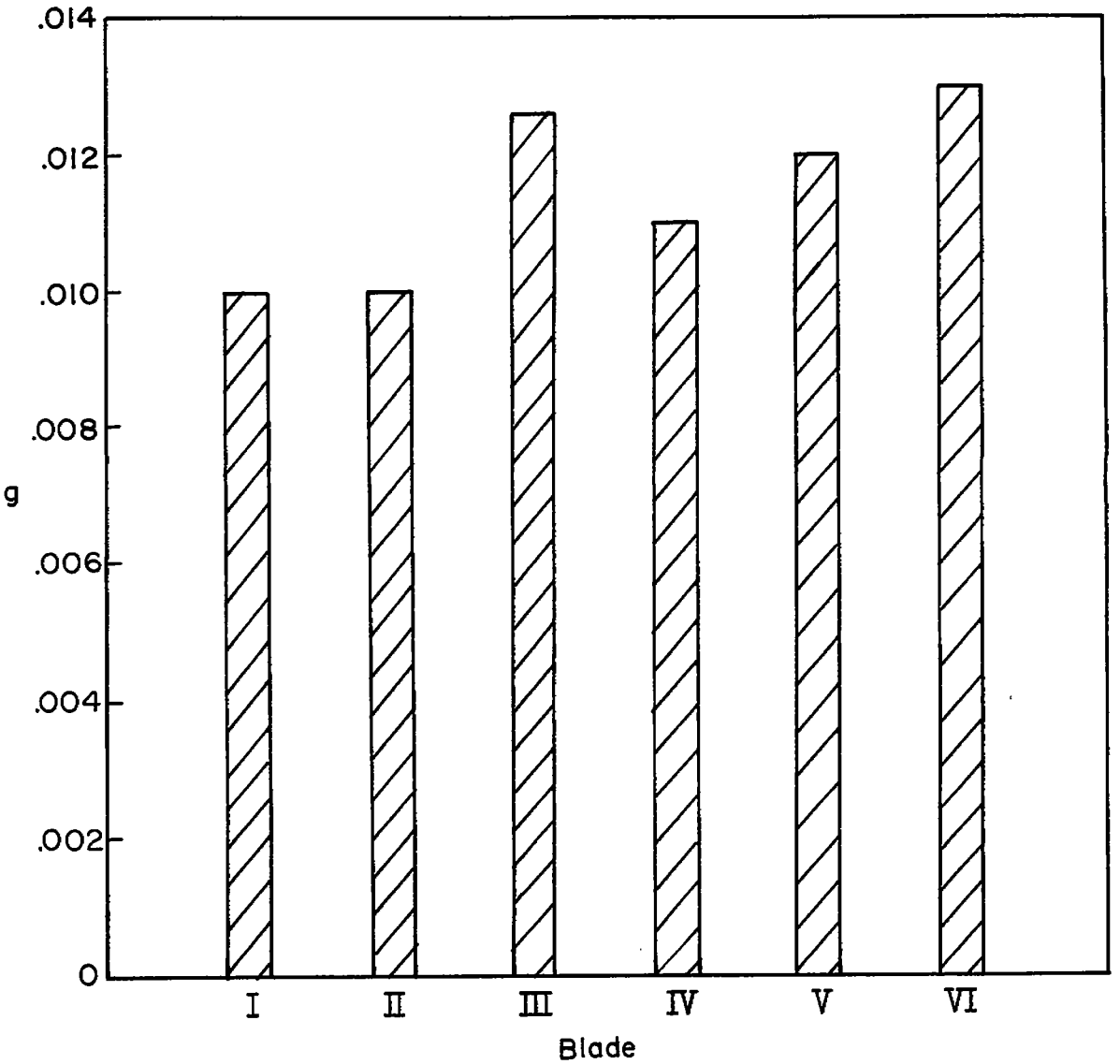

Figure 8.- Effect of material on the structural damping in the first flapwise bending mode.

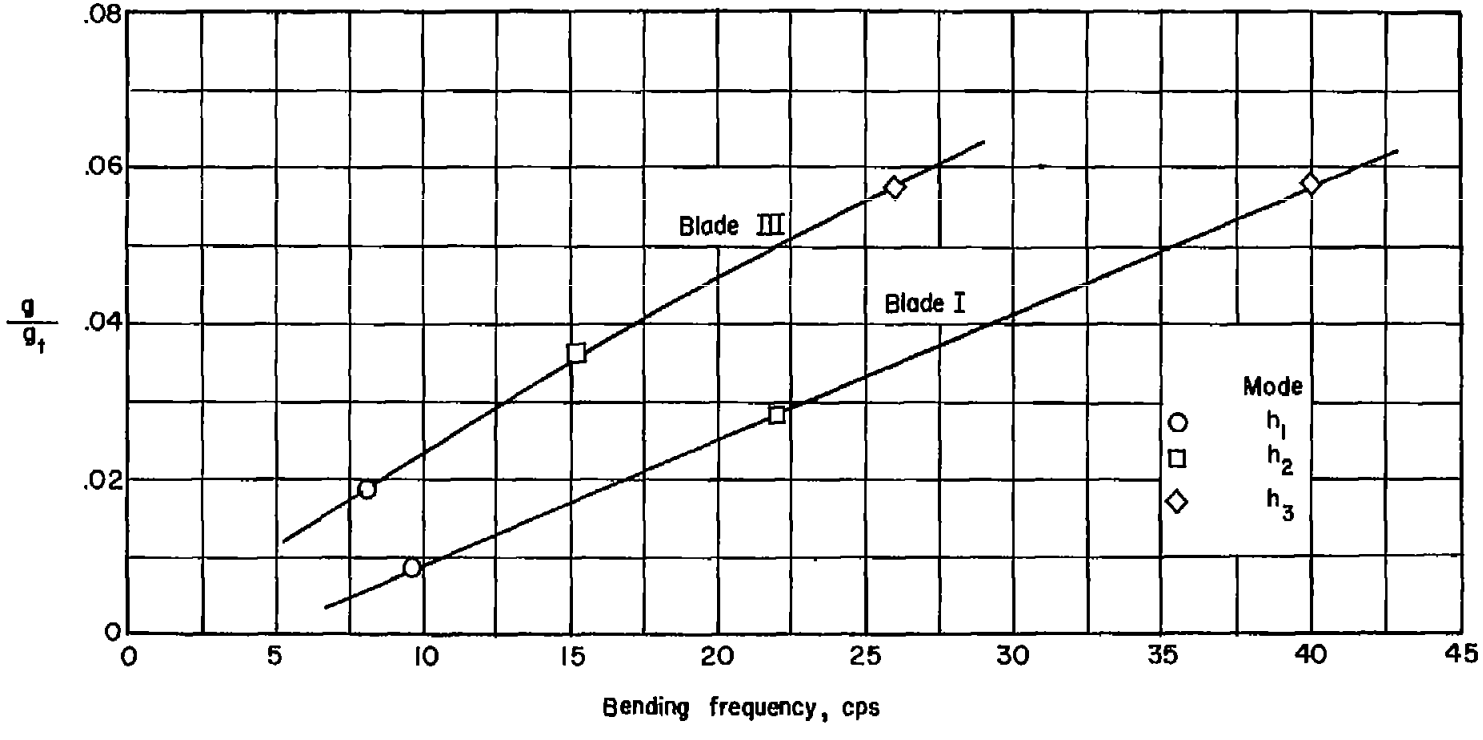

Figure 9.- Variation of the ratio of structural damping to total damping with bending frequency for two blades of different construction but with similar mass and stiffness distributions.

NACA - Langley Field, Va.